BMC Cancer

RESEARCH

Open Access

Impacts of combining PD-L1 inhibitor and radiotherapy on the tumour immune microenvironment in a mouse model of esophageal squamous cell carcinoma

Zihao Yin[1], Hongfang Zhang[2], Ke Zhang[1], Jing Yue[2], Rongjun Tang[3], Yaping Wang[4], Qinghua Deng[1*] and Qingqing Yu[1*]

Abstract

Background The combination of radiation with immune checkpoint inhibitors (ICIs) has been demonstrated to display synergistic effects in solid cancers. Nevertheless, the anti-tumor effect of combining radiation with programmed cell death 1 ligand 1 (PD-L1) inhibitor in esophageal squamous cell carcinoma (ESCC) has remained unclear. Therefore, the objectives of our study were to evaluate the anti-tumor effects of PD-L1 inhibitors combined with radiotherapy in a mouse model of ESCC and to depict the immune landscape within the tumor microenvironment (TME).

Methods Murine ESCC cells (mEC25) were injected subcutaneously into the right flanks of C57BL/6 mice. Tumor-bearing mice were exposed to different treatments: IgG antibody (control), anti-PD-L1 antibody, radiation, or radiation + anti-PD-L1 antibody. Tumor growth and survival time of mice were monitored. Tumour immune microenvironment was assessed by flow cytometry, including $CD4^+$T cells, $CD8^+$T cells, regulatory T cells (Tregs), tumor-associated macrophages (TAMs), myeloid-derived suppressor cells (MDSCs), and the activation and exhaustion of $CD8^+$T cell. In addition, transcriptomic analysis was used to examine the changes in immune gene expression in the TME.

Results Radiotherapy combined with anti-PD-L1 inhibitors (radioimmunotherapy) synergistically enhanced anti-tumor immune response, leading to decreased tumor growth and prolonged survival of tumor-bearing mice. The radioimmunotherapy increased the infiltration of $CD8^+$ T cells, the ratio of $CD8^+$ T cells to Tregs, the population of central memory $CD8^+$ T cells (T_{CM}), interferon-gamma (IFN-γ) secretion of tumor-infiltrating $CD8^+$ T cells, and reduced the accumulation of M2-type TAMs and Tregs in the TME in mouse model. In addition, the radioimmunotherapy induced anti-tumor immune response in the spleen and tumor-draining lymph node (TDLN). Moreover, transcriptomic analysis suggested that the radioimmunotherapy promoted the activation of immune regulatory pathways and increased the expression of cytokines such as CXCL9 and CXCL10, thus creating an immunoinflammatory tumor microenvironment.

Conclusions Our research revealed that anti-PD-L1 inhibitors combined with radiotherapy caused systemic anti-tumor immunity by reshaping the immune microenvironment in a mouse model of ESCC.

*Correspondence:
Qinghua Deng
dengqinghua69@163.com
Qingqing Yu
yuqq1983@163.com
Full list of author information is available at the end of the article

Keywords Programmed death ligand 1, Radiotherapy, Tumor microenvironment, Esophageal squamous cell carcinoma

Introduction

Esophageal squamous cell carcinoma (ESCC) is a common malignant tumor worldwide [1]. Due to the inconspicuous early symptoms and the lack of early diagnosis, ESCC is often diagnosed at advanced stages, and patients have a poor prognosis [2]. Definitive chemoradiotherapy is the current standard protocol for unresectable locally advanced ESCC. Previous studies have explored the optimal combination of chemotherapy and radiotherapy. However, the rates of local tumor recurrence have remained high, with 5-year overall survival rates of only 20%-25% [3–5].

Immune checkpoint inhibitors (ICIs) have been demonstrated as a prospective therapeutic strategy of treating ESCC patients. Several studies, including KEYNOTE-590 [6] and Escort-1st [7], have demonstrated that PD-1/PD-L1 monotherapy improved the survival of advanced ESCC patients, demonstrating reliable efficacy and a favorable safety. However, due to the heterogeneity of tumors immune microenvironment, only 20% of ESCC patients were responders of ICIs monotherapy. To overcome this limitation, several studies have been focused on the combination of immunotherapy and chemoradiotherapy.

Radiotherapy (RT) is used for treating all stages of ESCC. Furthermore, radiation has been proved to produce significant effects on the immune response of various types of tumors [8, 9]. Radiation induces immunogenic death of tumour cells and the production of tumour antigens, which function as in situ vaccines to activate systemic anti-tumour immune responses. Local radiation repressed tumor growth by promoting the recruitment of $CD8^+$ T cells and secretion of IFN-γ [10]. Furthermore, several studies have demonstrated that radiation increased the expression of PD-L1 on tumor cells [11], which may enhance tumor targeting of anti-PD-L1 immunotherapy [12, 13]. Conversely, ICIs can induce the activation of effector T cells to eliminate tumor cells and normalization of tumor vasculature, increasing lymphocyte infiltration and tumor sensitivity to radiotherapy [14, 15]. In summary, the combination of radiotherapy and immunotherapy may induce a synergetic effect on anti-tumor response. Previous studies have confirmed that radiotherapy in combination with PD-L1 inhibitors can induce synergetic antitumor effects in preclinical models of lung [16, 17], melanoma [18], colorectal cancer [12], breast cancer [12], head and neck squamous cell carcinoma(HNSCC) [19, 20], prostate cancer [21, 22], and pancreatic ductal adenocarcinoma(PDAC) [23].

Radiotherapy combined with anti-PD-L1 immunotherapy (radioimmunotherapy) has emerged as a prospective therapy for ESCC patients. However, their synergistic effect and molecular mechanisms in ESCC are not entirely understood. Therefore, our study aimed to evaluate the synergistic anti-tumor effect of radioimmunotherapy in an ESCC preclinical model and define the molecular mechanisms through depicting the immune landscape within the tumor microenvironment.

Materials and methods

Preparation of cell lines

The murine ESCC cell line mEC25 was purchased from Shenzhen Wenhua Times Technology Co., Ltd and cultured in RPMI-1640 medium (11,875,119, Gibco, CA, USA) with 10% fetal bovine serum (Gibco, Life Technologies Inc.) in a 5% CO_2 humidified incubator at 37℃.

In vivo studies

Female C57BL/6 mice (4–6 weeks old) were provided by the Laboratory Animal Center, Zhejiang Academy of Medical Sciences (Hangzhou, China). All mice were maintained and treated according to the institutional animal welfare guidelines of Zhejiang Academy of Medical Sciences. Mice were injected subcutaneously with 5×10^5 mEC25 cells on the right flank. When the volume of tumors reached 90–120 mm^3 (Day 1), the tumor-bearing mice were randomly divided into 4 groups and exposed to different treatments: Control (IgG antibody); RT(4Gy×3)+IgG antibody; Anti-PD-L1 antibody; RT(4Gy×3)+Anti-PD-L1 antibody. For radiation therapy (RT), tumors were irradiated in 3 fractions for a total dose of 12 Gy. RT was administered via an electron beam on day 1, 4, and 7. Briefly, mice were anesthetized and placed under a lead shield with a 1 cm^2 hole to ensure tumor exposure. Anti-PD-L1 antibody (BioXCell, clone 10F.9G2) or IgG antibody (BioXCell, rat IgG2b) was delivered by intra-peritoneal injection at a dose of 10 mg/kg alone or combined with radiotherapy at day 1, 4, and 7. We measured tumor size using calipers and calculated its volume using the formula (length×$width^2$/2), where length and width are the longest and shortest diameter of the tumor, respectively. Survival time of the mice was recorded. When tumor volume reached 1500 mm^3, or the tumor was ulcerated, the mice were subjected to

euthanasia due to significant tumor pain and the day was recorded as the survival time of mice. Based on the recommendations for euthanasia of experimental animals [24, 25], the mice were anesthetized by intraperitoneal injection of sodium pentobarbital solution (100mg/kg) and sacrificed by cervical dislocation.

Flow cytometry analysis

The tumor, spleen and tumor draining lymph nodes (TDLNs) of mice (three mice per group) were isolated on days 10 and 14. The tissues were cut into small pieces and incubated at 37°C for 30 min (tumor) or 10 min (TDLN) in RPMI medium with collagenase type IV and deoxyribonuclease type I and then mechanically separated on frosted slides. Spleens were mechanically separated directly on frosted slides. Single-cell suspension was obtained by filtering the cell suspension into a 70-μm cell strainer (Corning). A lysis buffer (NH4Cl, NaHCO3, EDTA) was used to lyse erythrocytes at room temperature and quenched with RPMI medium. Fixable Viability Stain 440UV (566,332, BD) and α-CD16/32 (553,142 BD) were used to label and block the cells.

For surface staining, monoclonal antibodies (Supplemental Table S1) were used to stain the samples for 30 min at room temperature. Each group was analyzed at least three replicates. The data were obtained based on FACSCalibur machines and analyzed using Flowjo software.

Intracellular staining

To assess the content of IFN-γ and granzyme B, the cell suspensions were stimulated with 1 μM phorbol 12- myristate 13- acetate (PMA, Sigma) and ionomycin (Sigma) for 4 h at 37 °C. Then, the cells were fixed and permeabilized with FOXP3 Fix/Perm Buffer Set (562,574, BD), and subsequently stained with monoclonal antibodies (Supplemental Table S1) for 30 min on ice following the manufacturer's instructions.

Immunohistochemistry (IHC)

4% paraformaldehyde was used to fix tumor tissues and paraffin was used to embed them. Sections were deparaffinized, rehydrated, antigenically repaired and stained overnight at 4 °C with the primary antibodies as follows: CD8 (D4W2Z, 98,941, Cytotoxic T cell), FOXP3 (D608R, 12,653, Regulatory T cell), CD206 (E6T5J, 24,595, M2-macrophage), CD86(E5W6H, 19,589, M1-macrophage), GZMB(13,588–1-AP, Cytotoxic T cell). The sections were then incubated with secondary antibodies and reacted with ABC kits (Vector, Burlingame, CA). Stained sections were observed using ECLIPSE E100 light microscope (NIKON) and K-Viewer software. Quantitative analysis of optical density was evaluated by Image J software (National Institutes of Health). The average density of 3 slices per sample was calculated.

RNA sequencing and bioinformatic analysis

The total RNA was extracted by Trizol Reagent (15,596,026, Thermo Fisher Scientific Inc., MA, USA). RNA sequencing (RNA-seq) assay was performed using the Illumina Hiseq 2500 platform. Musmusculus GRCm38 was the reference genome. Differentially expressed genes (DEGs) were screened using the edgeR package in R software. GO and KEGG 2018 databases were used for gene set enrichment analysis.

RNA extraction and quantitative real-time PCR (qRT-PCR)

The extraction of total RNA from tumor tissues was performed using Trizol Reagent. Reverse transcription was accomplished using PrimeScript™ RT Master Mix (RR036A, Takara Biomedical Technology (Beijing) Co., Ltd., Beijing, China). Quantitative RT-PCR (qRT-PCR) was carried out with TB green (RR420A, Takara Biomedical Technology Co., Ltd., Beijing, China). Furthermore, the mRNA expressions of targeted genes including CXCL9 and CXCL10 (the primers were listed in Supplemental Table S2) was calculated and normalized using $2^{-\Delta\Delta Ct}$ method.

Statistical analysis

One-way ANOVA analysis was used to perform statistical comparisons between three or more groups, followed by Tukey's multiple comparison test. For tumor volume, statistical analysis was performed using mixed-effects model with Tukey's multiple comparison test. Survival curves for different groups of mice were generated using the Kaplan- Meier method. The the log- rank Mantel-Cox test was used to evaluated the survival curves of mice in each group. Tumor volumes of at least three mice in each group were subjected to t-tests, and the results were expressed as mean ± standard error of the mean (SEM). $P < 0.05$ was regarded as statistically significant (*, $p < 0.05$; **, $p < 0.01$; ***, $p < 0.001$; ****, $p < 0.0001$). The statistical analyses were performed with GraphPad Prism statistical analysis and graphing software (GraphPad 9).

Results

Anti-PD-L1 inhibitors combined with radiotherapy synergistically enhanced anti-tumor effects in a mouse model of esophageal cancer

We demonstrated that fractionated radiotherapy increased the expression of PD-L1 on human esophageal cancer cell lines (Supplementary Fig. S1). Therefore, we aimed to explore whether anti-PD-L1 inhibitor combined with radiotherapy could synergistically reinforce anti-tumor

efficacy. We subcutaneously injected mEC25 murine cancer cells into syngeneic mice and the tumor-bearing mice were exposed to different treatment regimens including IgG antibody alone (control), anti-PD-L1 antibody alone, radiation therapy combined with IgG antibody and radiation therapy combined with anti-PD-L1 antibody (Fig. 1a). We found that the radioimmunotherapy (radiation therapy combined with anti-PD-L1 antibody) demonstrated the strongest inhibition of tumor growth (Fig. 1b). Radioimmunotherapy significantly slowed down tumor growth compared with RT ($p=0.008$), anti-PD-L1 ($p=0.01$) and control groups ($p=0.01$) (Fig. 1b). In addition, radioimmunotherapy also improved the survival time of tumor-bearing mice compared with RT ($p=0.0007$), anti-PD-L1 ($p=0.0248$) and control groups ($p=0.0001$) (Fig. 1c). Compared with 33 days for radioimmunotherapy, the median survival time for RT was 26 days, for anti-PD-L1 was 28 days and for control group was 24 days, respectively.

Radioimmunotherapy regulated T cell infiltration

To define the alterations of cell populations in tumor microenvironment after radioimmunotherapy, lymphocytes were collected from the tumor, spleen and tumor draining lymph nodes (TDLN) at Days 10 and 14, and analyzed using flow cytometry (Supplementary Fig. S3). The extent of tumor-infiltrating $CD8^+$ T cells was associated with suppression of tumor growth. In the tumor, at Day 14, radioimmunotherapy significantly enhanced the infiltration of $CD8^+$ T cells compared with RT and control groups (55.8% ± 2.9% radioimmunotherapy vs 35.1% ± 0.9% RT $p=0.0049$; vs 41.5% ± 2.8% control $p=0.0413$; Fig. 2a, b). In the spleen, there were no significant differences among the groups at any time point (Fig. 2b). In the TDLN at Day 10, radioimmunotherapy

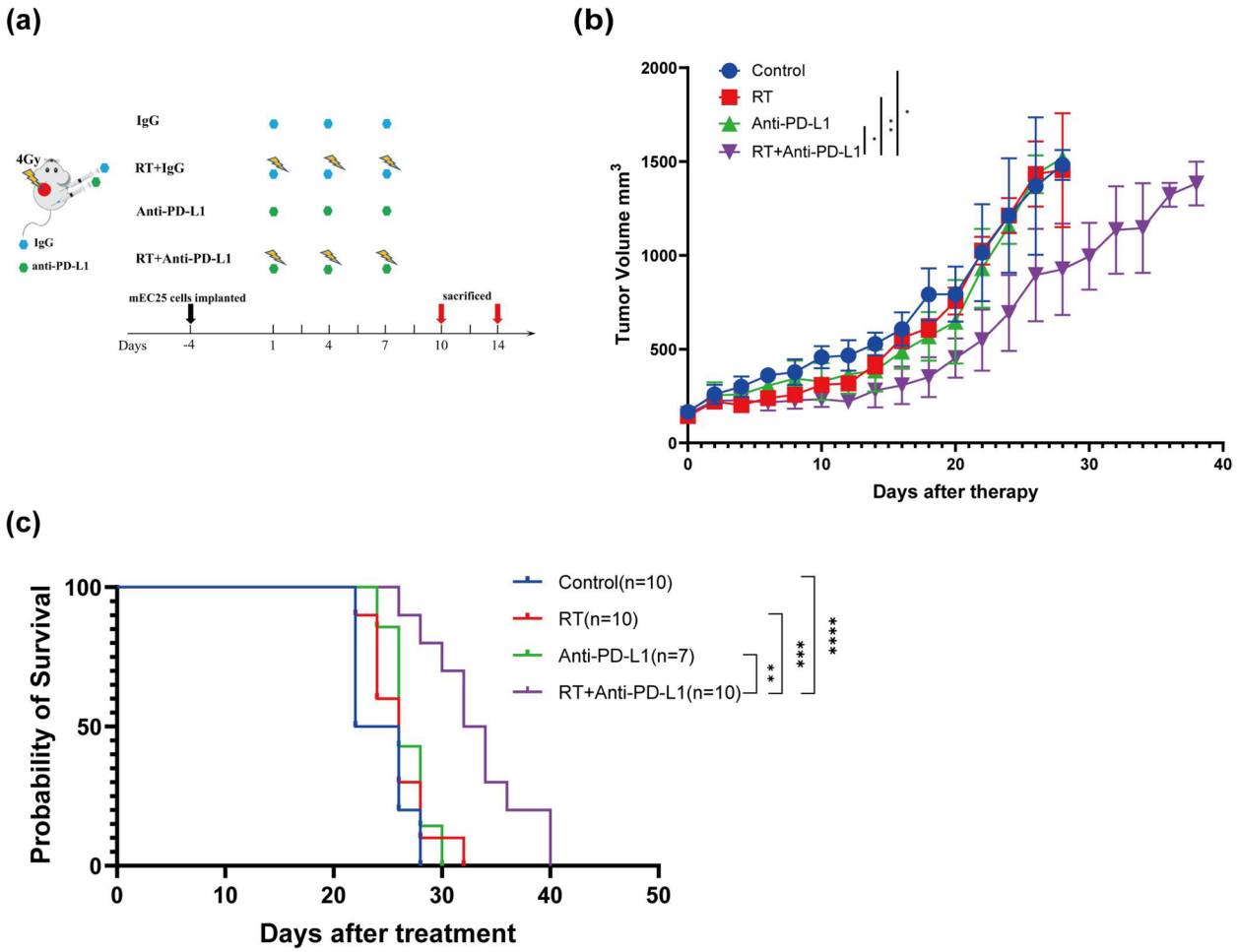

Fig. 1 Radioimmunotherapy inhibited tumor growth and improved survival time of tumor-bearing mice. **a** Schematic diagram of different treatments: IgG antibody (control), anti-PD-L1 antibody, radiation therapy (RT) or their combinations. **b** The changes of tumor volume in mice treated with different treatments. **c** Kaplan Meier survival curves of mice with different treatments. N = 10 in each group except for the group of anti-PD-L1 alone ($n=7$). (*$p<0.05$; **$p<0.005$; ***$p<0.0005$; ****$p<0.0001$)

increased the proportion of $CD8^+$ T cells compared with RT and control groups(39.8% ± 0.6% radioimmunotherapy vs 31.2% ± 3.1% RT $p = 0.0472$; vs 30.4% ± 0.2% control $p = 0.0316$; Fig. 2b). Meanwhile, there were no significant differences in the population of $CD4^+$ T cells at any time point in the tumor, spleen and TDLN following different treatments (Supplementary Fig. S2a). Therefore, we further investigated the impact of radioimmunotherapy specifically on the regulatory T (Treg) cells ($CD25^+FOXP3^+CD4^+$T cell), which are an immunosuppressive subset of $CD4^+$ T cells. In the tumor, at Day 14, radioimmunotherapy decreased the percentage of infiltrating Tregs compared with that in other groups (5.6% ± 0.6% radioimmunotherapy vs 13.8% ± 0.2% RT $p < 0.0001$; vs 8.4% ± 0.5% Anti-PD-L1 $p = 0.0105$; vs 12.3% ± 0.2% control $p < 0.0001$; Fig. 2c, d). The Anti-PD-L1 group also significantly reduced tumor-infiltrating Tregs compared with RT and control groups. In the spleen at Day 10, we found that radiation increased the proportion of Tregs compared with control group, suggesting that RT can induce the up-regulation of Tregs as an immunosuppressive regulator. Notably, radioimmunotherapy induced the lowest proportion of tumor-infiltrating Tregs (Fig. 2d). In addition, the proportion of Tregs was markedly reduced in anti-PD-L1 group compared with RT and control groups (Fig. 2d). In the TDLN, there were no significant differences between radioimmunotherapy and other groups at any time point.

We also investigated the ratio of $CD8^+$T cells/$Foxp3^+$Tregs. In the tumor, radioimmunotherapy increased the ratio of $CD8^+$T cells/Treg compared with that in other groups at Day 14(75.4 ± 18.1 radioimmunotherapy vs 14.6 ± 0.4 RT $p = 0.0105$; vs 25.7 ± 5.8 Anti-PD-L1 $p = 0.0305$; vs 20.1 ± 1.7 control $p = 0.0175$), with a same phenomenon seen in the spleen(90.8 ± 3.9 radioimmunotherapy vs 55.1 ± 7.5 RT $p = 0.0170$; vs 60.4 ± 7.3 Anti-PD-L1 $p = 0.0380$; vs 55.3 ± 5.8 control $p = 0.0175$) and TDLN(67.1 ± 2.8 radioimmunotherapy vs 39.9 ± 1.9 RT $p = 0.0003$; vs 46.5 ± 2.6 Anti-PD-L1 $p = 0.0022$; vs 53.0 ± 2.7 control $p = 0.0206$) at Day 14 (Fig. 2e). No significant differences were found at Day 10 in the tumor, spleen and TDLN. In addition, these results were consistent with the concomitant immunohistochemistry on day 14 (Fig. 2f). Therefore, these results demonstrated that radioimmunotherapy could increase the ratio of $CD8^+$ T cells/Tregs by improving the recruitment of $CD8^+$ T cells and reducing the accumulation of Tregs.

Radioimmunotherapy enhanced the activation of immune memory

We further investigated whether different treatments influenced the activation of immune memory. We defined the effector-memory phenotype of T cells as $CD44^+$ $CD62L^-$ populations, and central-memory T cells as $CD44^+$ $CD62L^+$ populations, respectively. Firstly, we analyzed $CD8^+$ T cells expressing CD44. CD44 is an activation marker of T cells after antigen stimulation. At Day 10 in the tumor, the percentages of $CD44^+CD8^+$ T cells in the group of radioimmunotherapy and anti-PD-L1 were lower than that in the group of RT and control. In the spleen, at Day 10, radioimmunotherapy increased the proportion of $CD44^+CD8^+$ T cells compared with other groups (48.2% ± 2.2% radioimmunotherapy vs 37.2% ± 1.9% RT $p = 0.031$; vs 36.8% ± 0.1% Anti-PD-L1 $p = 0.0257$; vs 32.1% ± 3.2% control $p = 0.0046$; Fig. 3a). Moreover, radioimmunotherapy enhanced the proportion of $CD44^+CD8^+$ T cells compared with RT and control groups at Day 14($p < 0.0001$). In the TDLNs, radioimmunotherapy increased the percentage of $CD44^+CD8^+$ T cells compared with RT and control groups at Day 10 ($p = 0.0391$; $p = 0.0356$, respectively). At Day 14, radioimmunotherapy increased the percentage of $CD44^+CD8+$T cells compared with anti-PD-L1 and control groups ($p = 0.0316$; $p = 0.0002$, respectively; Fig. 3a).

For central-memory $CD8^+$ T cells (T_{CM}), in the tumor, we found that radioimmunotherapy enhanced the accumulation of $CD8^+$ T_{CM} at Day 14 compared with those in other groups (10.3% ± 0.2% radioimmunotherapy vs 2.5% ± 0.1% RT $p < 0.0001$; vs 5.5% ± 0.4% Anti-PD-L1 $p < 0.0001$; vs 3.3% ± 0.1% control, $p < 0.0001$; Fig. 3b, c). In the TDLN at Days 10 and 14, the same trends were also observed (Day 10: 11.1% ± 0.5% radioimmunotherapy vs 5.8% ± 0.9% RT $p = 0.0011$; vs 6.7% ± 0.5% Anti PD-L1 $p = 0.0035$; vs 6.1% ± 0.4% control $p = 0.0014$; Day 14: 13.8% ± 0.8% radioimmunotherapy vs 9.8% ± 0.3% RT $p = 0.0087$; vs 3.2% ± 0.4% Anti PD-L1 $p < 0.0001$; vs 2.3% ± 0.6% control $p < 0.0001$; Fig. 3b, c). In the spleen, compared with Anti-PD-L1 and control groups at Day

(See figure on next page.)

Fig. 2 Radioimmunotherapy regulated T cell infiltration. **a** Representative plots of $CD8^+CD3^+$ T cells in tumors at Day 14. **b** Quantification of infiltrating $CD8^+$ T cells at Days 10 and 14 in tumor, spleen and TDLN. **c** Representative plots of $CD25^+FOXP3^+$ Treg in tumors at Day 14. **d** Quantification of $CD25^+FOXP3^+$ Treg in the tumor, spleen and TDLN at Days 10 and 14. **e** Quantification of the ratio of $CD8^+$ T cells/$CD25^+FOXP3.^+$Treg at Days 10 and 14 in the tumor, spleen and TDLN. **f** Representative immunohistochemistry images of CD8 and FOXP3 expression in tumors from each group at Day 14. The original magnification was 200× ($n = 3$ mice each group). (*$p < 0.05$; **$p < 0.005$; ***$p < 0.0005$; ****$p < 0.0001$)

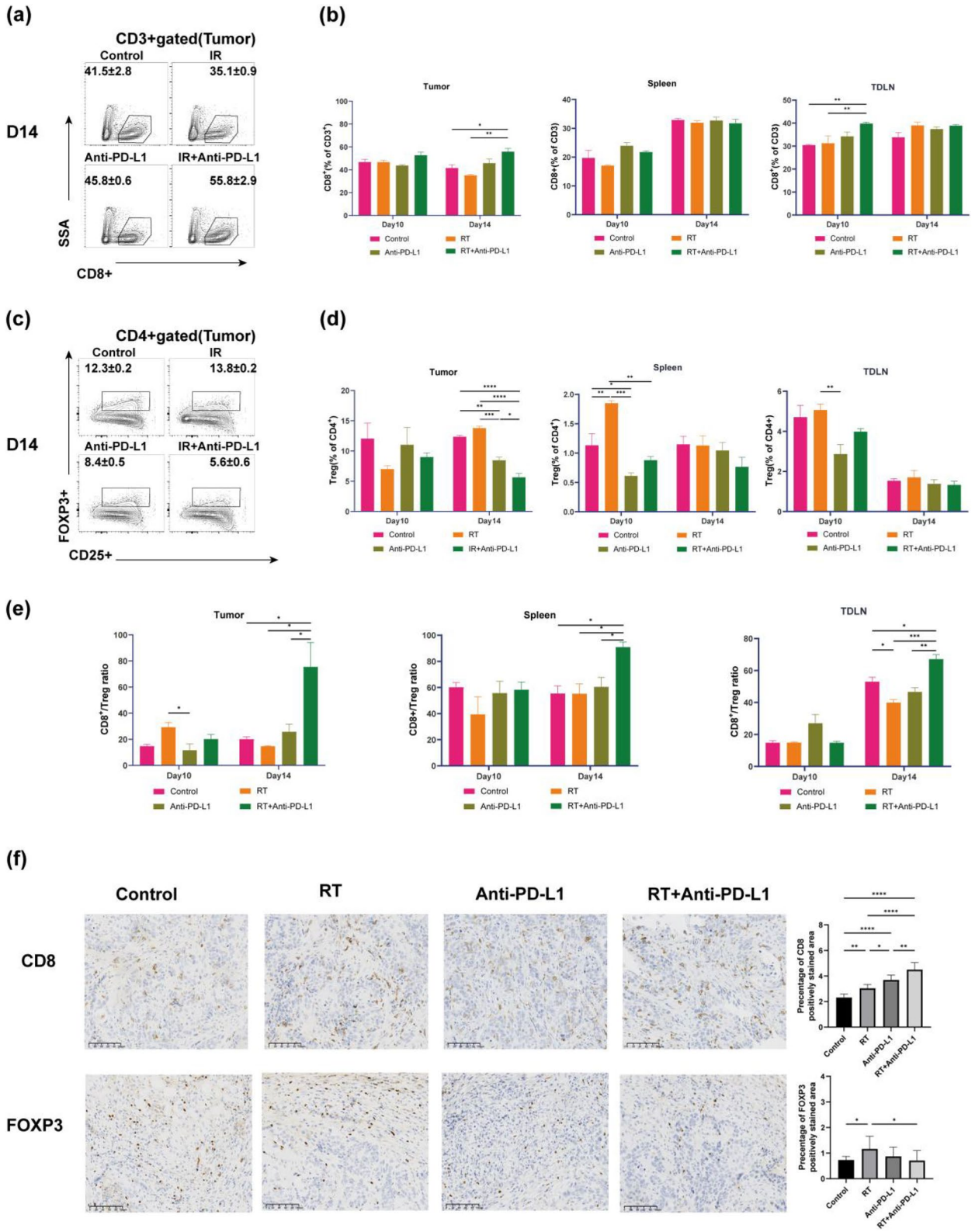

Fig. 2 (See legend on previous page.)

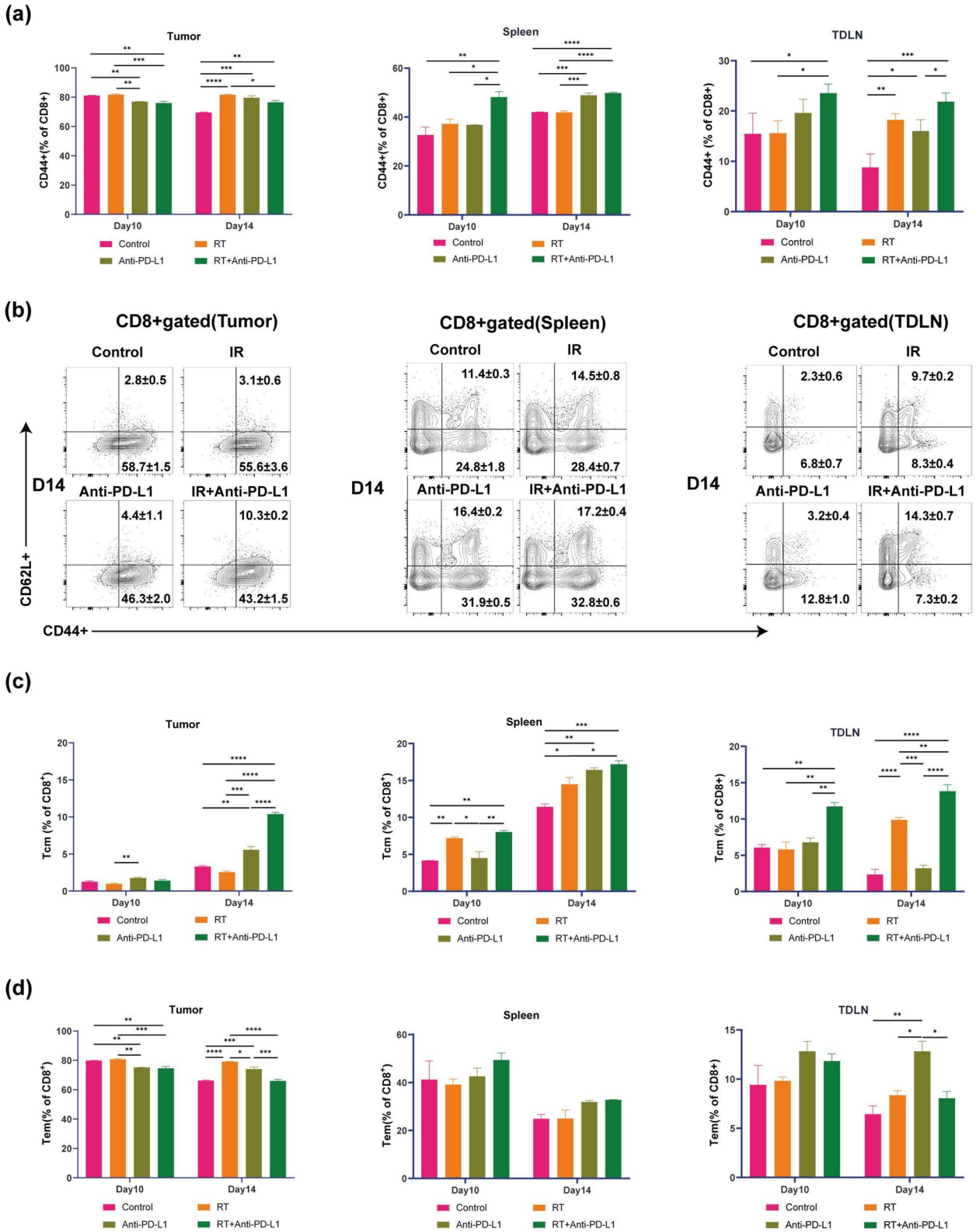

Fig. 3 Radioimmunotherapy promoted the activation of immune memory. **a** Quantification of infiltrating $CD44^{+}CD8^{+}$ memory T cells at Days 10 and 14 in the tumor, spleen and TDLN. **b** Representative graphs of CD62L and CD44 expression on $CD8^{+}$ T cells at Day 14 in the tumor, spleen and TDLN. **c** Quantification of infiltrating $CD8^{+}T_{CM}$ ($CD62L^{+}CD44^{+}$) cells and **d** $CD8^{+}T_{EM}$ ($CD62L^{-}CD44.^{+}$) cells at Days 10 and 14 in the tumor, spleen and TDLN. (*$p < 0.05$; **$p < 0.005$; ***$p < 0.0005$; ****$p < 0.0001$)

10, radioimmunotherapy increased the filtration of $CD8^+T_{CM}$ cells ($p=0.0022$; $p=0.0012$, respectively). At Day 14, compared with RT and control groups, radioimmunotherapy significantly increased the infiltration of $CD8^+T_{CM}$ cells ($p=0.0368$; $p=0.0004$, respectively; Fig. 3b, c). These results indicated that radioimmunotherapy can increase the proportion of $CD8^+T_{CM}$ cells.

For infiltrating $CD8^+$ effector-memory T cells (T_{EM}), in the tumor, we observed the same phenomenon consistent with $CD44^+CD8^+$ T cells at Days 10 and 14. In the spleen, no statistical significances were observed. In the TDLN, the proportion of $CD8^+T_{EM}$ cells were higher in the anti-PD-L1 group compared with other groups at Day 14 (Fig. 3d).

Radioimmunotherapy promoted cytotoxic functions of effector $CD8^+$ T cells

Additionally, we evaluated the cytotoxic functions of the effector $CD8^+$ T cells by detecting the expressions of IFN-γ and Granzyme B (GZMB). In the tumor, at Day 10, a significant increase in the proportion of IFN-γ^+CD8^+ T cells was observed in the radioimmunotherapy group compared with that in the RT and control groups ($p=0.0047$, $p=0.0013$, respectively, Fig. 4a, b). Similarly, we observed the same phenomenon in the spleen at Day 14. Moreover, radioimmunotherapy induced a significantly higher proportion of IFN-γ^+CD8^+ T cells compared with other groups in the tumor at Day 14(45.9% ± 0.4% radioimmunotherapy vs 23.9% ± 0.3% RT $p<0.0001$; vs 25.6% ± 0.2% Anti-PD-L1 $p<0.0001$; vs 37.5% ± 0.2% control $p<0.0001$; Fig. 4a, b). Meanwhile, similar phenomenon was observed in the spleen at Day 10 and TDLN at Day 14 (Fig. 4a, b). Furthermore, we also detected the GZMB expression of $CD8^+$ T cells. At Day 10 in the tumor, a significantly increased proportion of $CD8^+$ T cells expressing GZMB occurred in the radioimmunotherapy group compared with that in other groups (31.6% ± 0.3% radioimmunotherapy vs 11.0% ± 0.2% RT $p<0.0001$; vs 18.7% ± 0.1% Anti-PD-L1 $p<0.0001$; vs 12.7% ± 0.2% control $p<0.0001$; Fig. 4c). Similar phenomenon was observed in the TDLN at Day 10 and tumor at Day 14. Meanwhile, we observed the same phenomenon at Day 14 in the tumor by flow cytometry and immunohistochemistry (Fig. 4c, d). There were no significant differences in the spleen (Fig. 4c). In summary, radioimmunotherapy can enhance the cytotoxicity of effector $CD8^+$ T cells.

Radioimmunotherapy influenced the expression of PD-1 on tumor-infiltrating $CD8^+$ T cells

We subsequently evaluated the PD-1 expression on tumor-infiltrating $CD8^+$ T cells. In the tumor, compared with control group, we found that radioimmunotherapy caused higher proportion of PD-1^+CD8^+ T cells at Day 14 ($p=0.0365$; Fig. 5e). The same phenomenon was observed at Day 10 in the spleen. No differences were observed in the TDLN. In addition, radioimmunotherapy notably enhanced the proportion of PD-1^+CD4^+ T cells in the tumors at Day 10 compared with those in other groups (Supplementary Fig. S2b). And no differences were observed in the spleen and TDLN. Taken together, radioimmunotherapy led to the highest proportion of $CD8^+$ and $CD4^+$ T cells expressing PD-1.

Radioimmunotherapy inhibited the recruitment of immunosuppressive cells

In addition to Tregs, we also investigated other immunosuppressive cells such as tumor-infiltrating mononuclear myeloid-derived suppressor cell (MDSCs, $CD11b^+Gr1^+CD45^+$) and tumor-associated macrophages (TAMs, $CD11b^+F4/80^+CD45^+$). In the tumor, radioimmunotherapy significantly reduced the percentage of immunosuppressive M2-TAMs compared with RT and anti-PD-L1 groups at Day 10 ($p=0.0231$, $p=0.0476$, respectively). Radioimmunotherapy also reduced the percentage of M2-TAMs in the tumor compared with that in other groups at Day 14 (2.1% ± 0.3% radioimmunotherapy vs 13.0% ± 0.7% RT $p=0.0141$; vs 17.1% ± 3.6% Anti-PD-L1 $p=0.0020$; vs 11.4% ± 0.3% control $p=0.0314$; Fig. 5a). A similar trend was also observed in the spleen at Day 14 (radioimmunotherapy vs RT $p=0.0469$; vs Anti-PD-L1 $p=0.0095$; vs control $p=0.0024$). In the TDLN, we found that radioimmunotherapy and anti-PD-L1 groups decreased the percentage of M2-TAMs compared with the RT and control groups at Days 10 and 14 (Fig. 5a). In addition, we measured the expressions of CD206 (M2-TAM marker) and CD86 (M1-TAM marker) in the tumor tissues at Day 14 by immunohistochemistry. And, the expression of PD-L1 on tumor tissues in control group at Day 14 was

(See figure on next page.)

Fig. 4 Radioimmunotherapy promoted the functions of effector $CD8^+$ T cells and increased PD-1 expression on $CD8^+$ T cells. **a** Representative graphs of IFN-γ^+CD8^+ T cells in tumors, spleen and TDLNS at Day 14. **b** Quantification of IFN-γ^+CD8^+ T cells in tumors, spleen and TDLN at Days10 and 14. **c** Quantification of $GZMB^+CD8^+$ T cells in tumors, spleen and TDLN at Days 10 and 14. **d** Representative images of GZMB by immunohistochemistry analysis in tumors at Day 14 from each group. **e** Quantification of PD-$1^+CD8.^+$ T cells in the tumor, spleen, and TDLN at Days 10 and 14. (*$p<0.05$; **$p<0.005$; ***$p<0.0005$; ****$p<0.0001$)

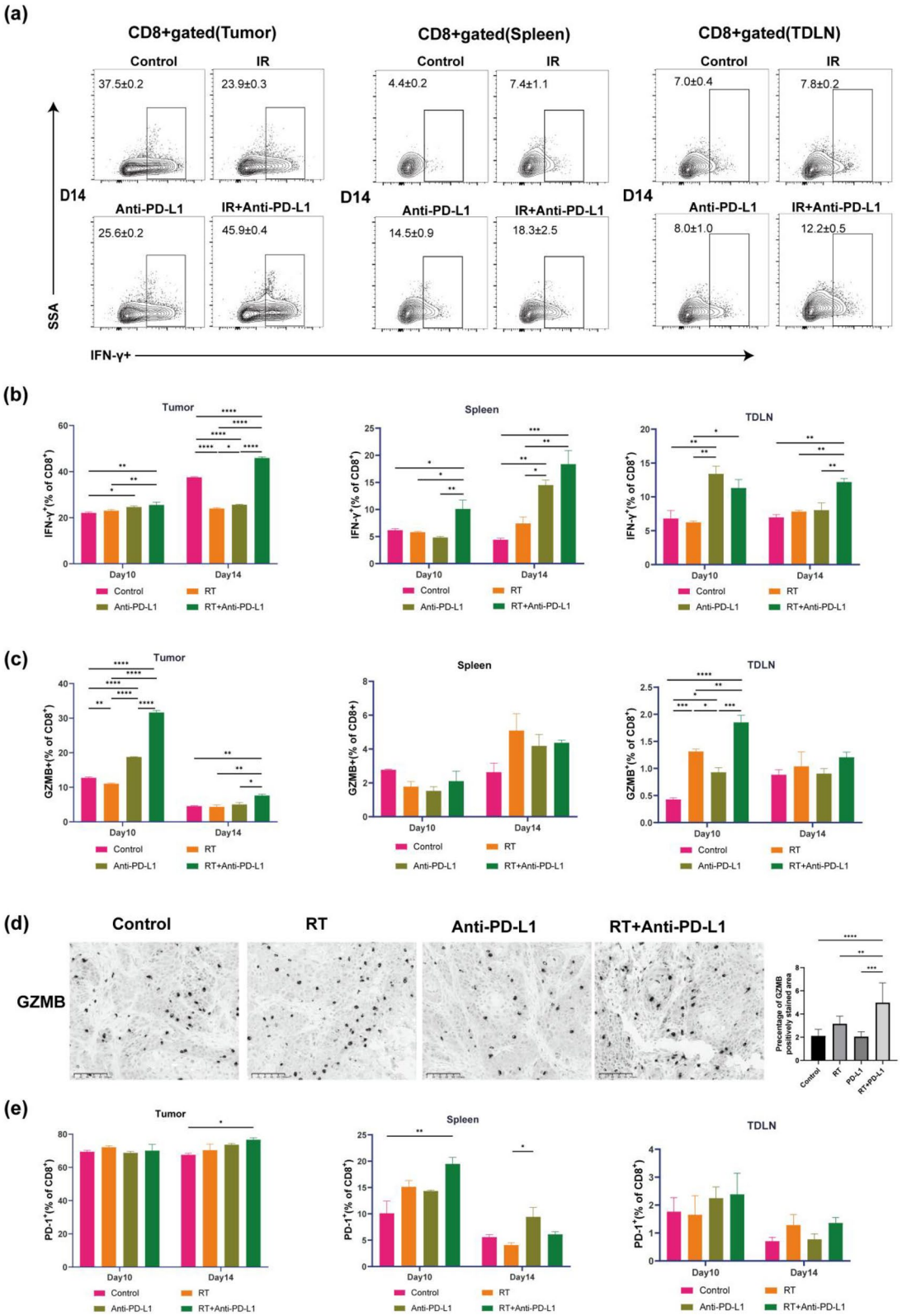

Fig. 4 (See legend on previous page.)

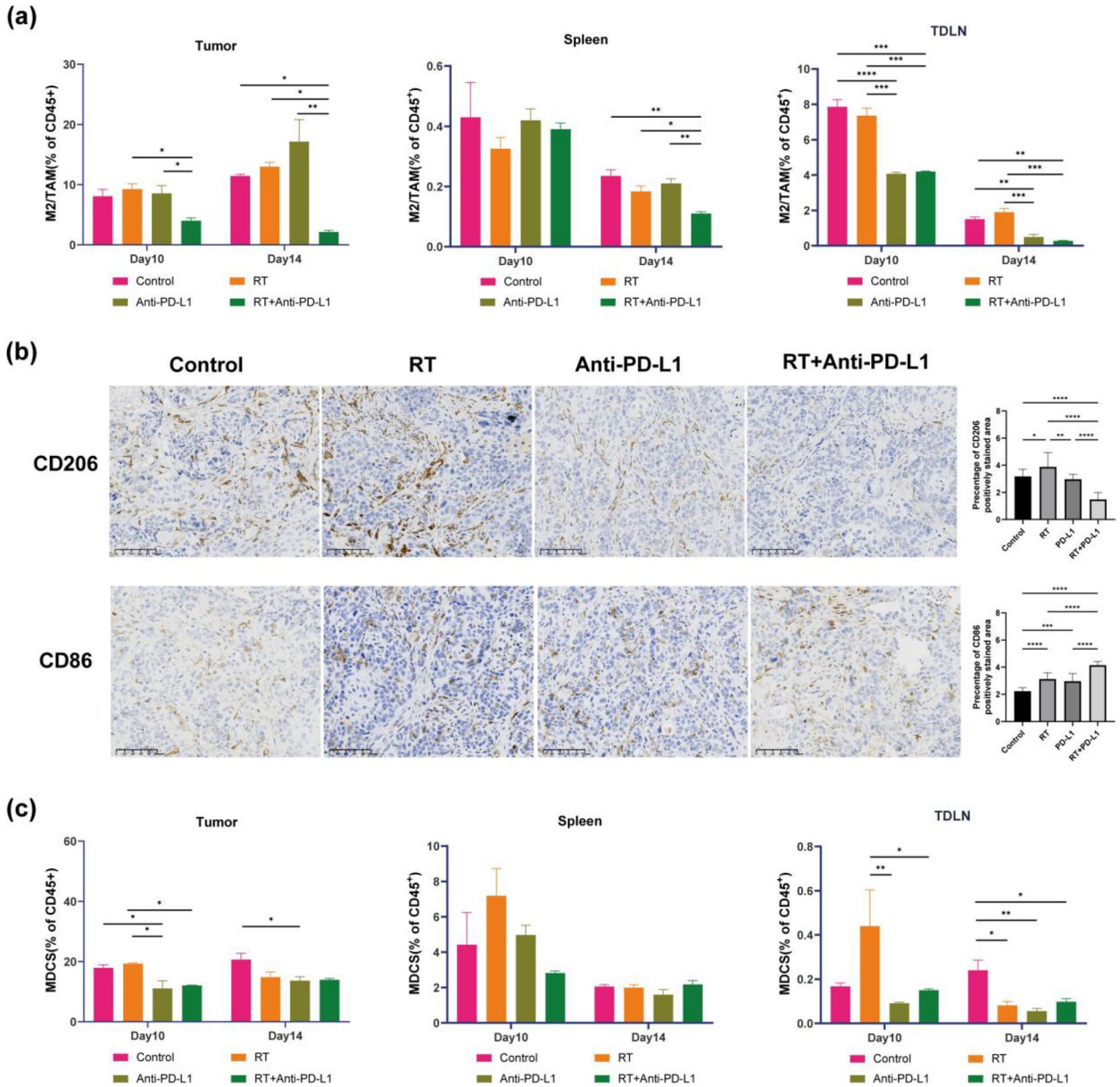

Fig. 5 Radioimmunotherapy inhibited the recruitment of several types of immunosuppressive cells. **a** Quantification of M2-TAM in the tumor, spleen and TDLN at Days 10 and 14. **b** Representative images of CD206 and CD86 by immunohistochemistry analysis in tumors at Day 14 from each group. **c** Quantification of MDSCs in the tumor, spleen and TDLN at Days 10 and 14. ($*p < 0.05$; $**p < 0.005$; $***p < 0.0005$; $****p < 0.0001$)

shown in Supplementary Fig. S4. We found the radioimmunotherapy group had the highest proportion of M1-TAMs (anti-tumor) and the lowest proportion of M2-TAMs (pro-tumor) compared with other groups (Fig. 5b). These results indicated that the radioimmunotherapy may inhibit the proliferation of M2-TAM. In addition, compared with RT group, radioimmunotherapy and anti-PD-L1 significantly decreased tumor-infiltrating MDSCs in the tumor and TDLN at Day 10 (Fig. 5c). No differences were observed in the spleen.

Radioimmunotherapy elicited an immunostimulatory tumor microenvironment

In our study, RNA-seq was used to systemically analyze transcriptome changes in the tumors following different treatments. Radioimmunotherapy-induced most

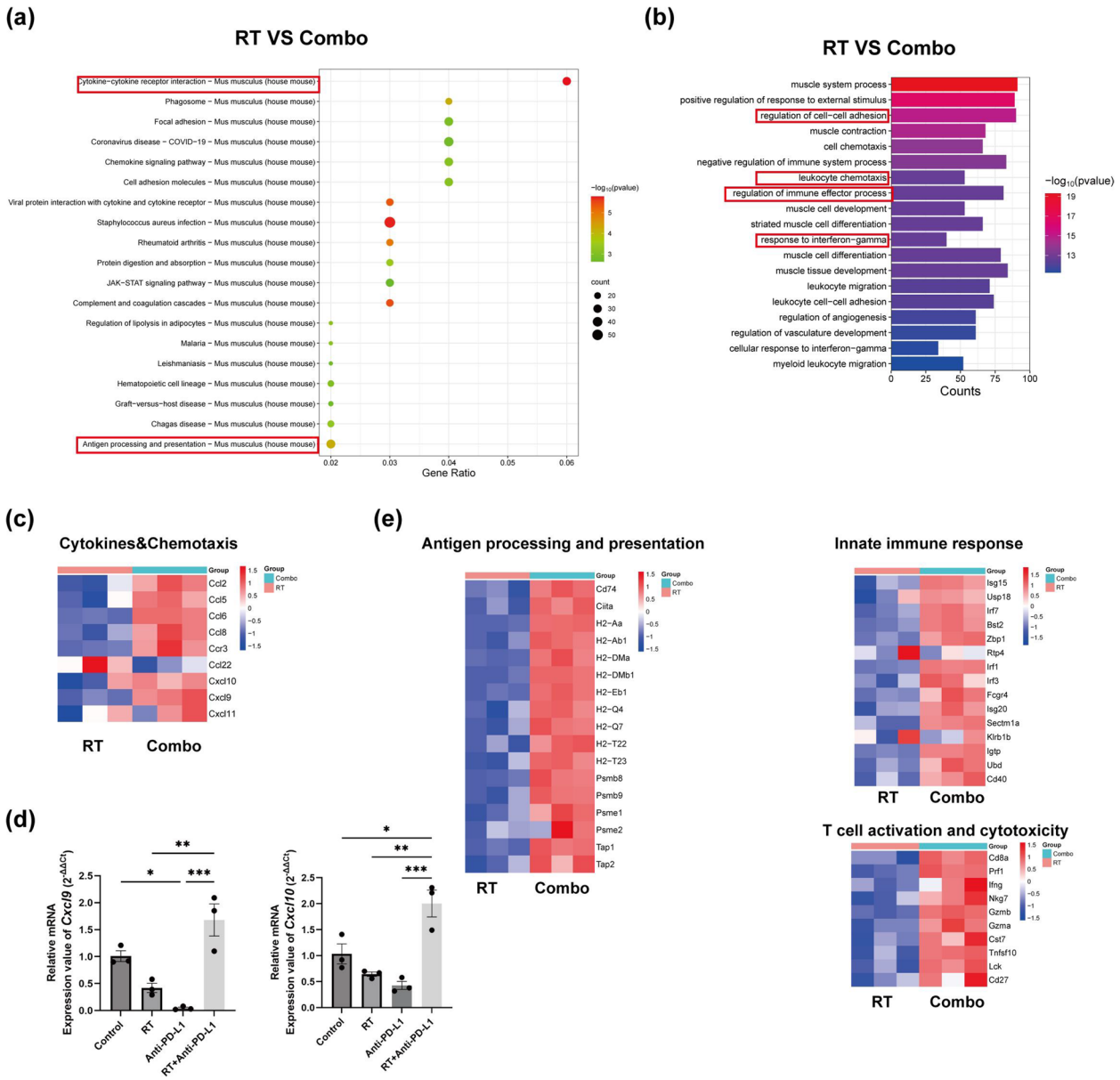

Fig. 6 Radioimmunotherpy induced an immunestimulatory antitumor microenvironment. **a** The enrichment of gene by KEGG pathways between radiation group and radioimmunotherapy groups. **b** GO analysis of top upregulated pathways in radioimmunotherapy group compared with radiation group. **c** Heatmap of enriched genes between radiation group and radioimmunotherapy groups in cytokine-cytokine receptor interaction and chemokine signaling pathway. **d** The mRNA expression of Cxcl9 and 10 genes in tumor mass. **e** Heatmap showing the expression of immunomodulatory genes in mEC25 tumor samples for radiation and radioimmunotherapy groups, such as regulating antigen processing and presentation genes, immune activation and cytotoxicity of T cells and innate immune response. The intensity of the heatmap represents z-scores. Data was analyzed using RNA-seq 14 days after irradiation ($n = 3$ mice per group). $^{*}p < 0.05$, $^{**}p < 0.01$, $^{***}p < 0.001$ with an unpaired two- tailed t- test

significantly enriched signaling pathways including cytokine-cytokine receptor interaction, chemokine signaling pathway and antigen processing and presentation genes were displayed in Fig. 6a. In addition, compared with the RT group, the tumors treated with radioimmunotherapy showed the most profound changes in pathways such as "regulation of cell–cell adhesion", "regulation of immune effector process" and "response to IFN-gamma" (Fig. 6b). Next, we observed that the expressions of chemokines involved in the attraction of T cells (eg, CXCL9, CXCL10 and CXCL11) were increased in the tumor in the radioimmunotherapy

group (Fig. 6c). We subsequently evaluated the expressions of CXCL9 and CXCL10 in tumor sites by qRT-PCR. Compared with other groups, radioimmunotherapy significantly increased the expressions of CXCL9 and CXCL10 (Fig. 6d). These data indicated that radioimmunotherapy can enhance the production of chemokines downstream of IFN-γ. In addition, we found antigen presentation-associated genes (MHC-I/II and Tap1/2), immune killing genes (Prf1, Ifn-γ, Gzma, and Gzmb) and innate immunity genes (Irf7, Isg15, Usp18) were all up-regulated in the radioimmunotherapy group (Fig. 6e). Taken together, these data demonstrated that the radioimmunotherapy can trigger both innate and adaptive immune response, creating an immunostimulatory tumor microenvironment.

Discussion

In our study, we demonstrated that anti-PD-L1 treatment combined with radiotherapy resulted in better tumor control and prolonged survival time of tumor-bearing mice. Importantly, we demonstrated that radioimmunotherapy stimulated $CD8^+$ T cell infiltration, improved the activity of effector $CD8^+$ T cell, increased the infiltration of $CD8^+T_{CM}$ and reduced the accumulation of M2-TAMs and Tregs, therefore reshaping an immune-stimulating tumor microenvironment and improving the anti-tumor efficacy in the mouse model of ESCC. Similar changes were also observed in the spleen and TDLN. To our knowledge, this is the first preclinical research depicting the synergistic anti-tumor immunity induced by the combination of anti-PD-L1 antibody and radiation in ESCC. Our findings were consistent with previous preclinical reports demonstrating synergistic anti-tumor effect induced by the combination of radiation and PD-L1 inhibitors in breast [12], colorectal [12], prostate cancer [21, 22], PDAC [23] and HNSCC [19, 20].

Our results showed that radioimmunotherapy can increase the proportion of IFN-γ^+ $CD8^+$ T cells. These results are consistent with previous studies in mouse lung and bladder cancer models [13, 26]. IFN-γ is essential for tumor control by cytotoxic $CD8^+$ T cells through inducing anti-tumor immunity in the murine models [27, 28]. Meanwhile, our data also showed that CXCL9 and 10 induced by IFN-γ stimulation were up-regulated in the radioimmunotherapy group. These changes are also reported by Alexis et al. and Oweida et al. in their preclinical models of bladder cancer and head and neck squamous cell carcinoma, respectively [20, 26]. The elevated levels of CXCL9 and CXCL10 were associated with recruiting anti-tumor $CD8^+$T cells and increased activation and cytotoxic responses of $CD8^+$ T cells [29–31]. The expressions of IFN-stimulated genes (Irf7, Isg15, Usp18) were increased in the radioimmunotherapy group. Notably, type I IFN stimulates antigen-presenting cells (APCs) to deliver tumor antigens for maintaining $CD8^+$T cell activation [10, 32]while suppressing Treg function to reinforce antitumor efficacy [33, 34]. Overall, radioimmunotherapy reprogrammed an immunostimulatory tumor microenvironment compared with anti-PD-L1 antibody or radiotherapy alone. In addition, radioimmunotherapy increased the GZMB content of $CD8^+$ T cells, indicating that radioimmunotherapy augmented the cytotoxicity of $CD8^+$ T cells. In summary, radioimmunotherapy promoted the recruitment and tumor-killing ability of $CD8^+$T cells and, importantly, induced the establishment of immunostimulatory tumor microenvironment.

Moreover, our results showed that radioimmunotherapy inhibited regulatory T cells (Tregs). It is known that Tregs significantly inhibit the functions of effector T cells. Several studies have reported that radiation recruited immunosuppressive Tregs in multiple murine tumor models, including melanoma, B cell lymphoma, and prostate cancer [11]. In a mouse model of pancreatic ductal adenocarcinoma, Azad et al. revealed that RT in combination with anti-PD-L1 inhibitor significantly reduced the infiltration of Tregs [23]. Consistent with their findings, our study also proved that radioimmunotherapy increasing $CD8^+$TILs/Treg ratio through promoting infiltration of $CD8^+$T cells and inhibiting Tregs accumulation, therefore improving anti-tumor immunity. The $CD8^+$TILs /Treg ratio has been recognized as a predictor of tumor response to immunotherapy [35, 36]. These results are in concordance with the results of Gong et al. in a mouse model of lung cancer [17].

M2-type macrophages promote immune tolerance, tumor invasion and metastasis [37]. Previous studies showed that radiation can recruit M2-type macrophages, thereby limiting radiation-induced adaptive anti-tumor immunity [38]. In addition, PD-L1 on the surface of macrophages binds to PD-1 on T cells, thereby inhibiting the co-stimulation of T cells by macrophages and resulting in T cell incompetence [39]. Xiong et al. reported that PD-L1 blockade induced IFN-γ secretion of $CD8^+$ T cells, promoting M1 polarization of macrophages in a mouse model of colon cancer [37]. Moreover, Jones et al. demonstrated that macrophage exhaustion partially attenuated immunosuppression after radiotherapy and additional anti-PD-L1 therapy was essential to accomplish tumor remission [40]. In our study, we found that only radioimmunotherapy significantly reduced the proportion of M2-type TAMs, which may be due to that only combination treatment increased the expression level of IFN-γ on $CD8^+$ T cells.

MDSC can inhibit T cell function and promote tumor immune escape [17]. The previous studies have

demonstrated that the combination of anti-PD-L1 and RT eventually resulted in a decreased amount of MDSC and PD-L1^{+}MDSCs in the irradiated and non-irradiated tumor tissues of breast, colorectal [12], lung [16] and pancreatic [23]. In agreement with these reports, we found that both radioimmunotherapy and anti-PD-L1 blockade inhibited MDSC recruitment in the TME at early time points, indicating that the addition of PD-L1 inhibitor attenuated the immunosuppressive effects of radiotherapy. Therefore, radioimmunotherapy reshaped the immune-stimulated microenvironment by eliminating immunosuppressive cells and promoting CD8^{+}T cells infiltration in TME.

T_{CM} cells are characterized by self-renewal and long-term survival in vivo. They can be rapidly differentiated into effector T cells following tumor antigens stimulation [41]. Several researchers have revealed that combining radiotherapy with ICIs could increase the account of CD8^{+} T_{CM} and inhibit tumor recurrence [41, 42]. We demonstrated that the proportion of infiltrating CD8^{+} T_{CM} cells was highest in the radioimmunotherapy group in TME, spleen, and TDLN, which may prevent or delay tumor recurrence.

T cell exhaustion is inevitable due to the continuous stimulation of tumor antigens. In our study, radioimmunotherapy increased the infiltration of PD-1^{+}CD8^{+}T cells, which was consistent with the findings of Dudzinski et al., indicating that radioimmunotherapy increased tumor antigen presentation and CD8^{+}T cell depletion [21]. Blackburn et al. have identified and separated the exhausted PD-1^{+}CD8^{+}T cells(T_{ex}) population into PD-1^{int} and PD-1^{hi} subsets during chronic viral infection in mice [43]. Moreover, previous studies have demonstrated that PD-1^{int}CD8^{+}T_{ex} could proliferate as the primary responders to anti-PD-1/PD-L1 inhibitors. On the contrary, the PD-1^{hi} subset more easily transferred into the terminal exhausted phenotype [43–45]. Moreover, compared with PD-1^{high} cells PD-1^{int} CD8^{+} T cells produced more amount of IFN-γ and GzmB upon restimulation [46]. However, in our study, we regret that we could not analyze the association between PD-1 expression and CD8^{+} T cell functions. In the future study, we will deeply explore their association.

Our studies also revealed the dynamic changes of immune cells in the spleen and TDLN. In the spleen and TDLN, radioimmunotherapy increased the infiltration of IFN-γ^{+}CD8^{+} T cells, CD8^{+}TILs/Treg ratio and the proportion of CD8^{+}$T_{CM,}$ and inhibited the recruitment of M2-type TAM, thus creating a systemic immune response. Due to the memory T cells in the spleen, the addition of PD-L1 blockade can significantly increase the percentage of effector CD8^{+}T-memory cells in LLC mouse model [16]. Some studies have demonstrated TDLN as an important source of anti-tumor immune cells, and alleviating immunosuppression in TDLN can promote systemic anti-tumor T cell immunity. Therefore, TDLN is essential in the anti-tumor immune response of radioimmunotherapy by increasing CD8^{+} T cell accumulation as well as M1/M2 macrophage ratio [47, 48]. Our results demonstrated that the synergistic effects of PD-L1 blockade combined with radiation in the spleen and TDLN may enhance the anti-tumor immune response by eliciting the abscopal effect.

However, there are some limitations associated with our study. First, the combination therapy did not completely eliminate the transplanted tumors in the mice. We agree with the opinion of Philippou et al. [22] that the radiation dose of 3×4Gy did not produce enough CD8^{+} T cell-dependent anti-tumor response. Therefore, it is essential to define the optical radiation dose and number of fractions when combined with anti-PDL1 immunotherapy. In addition, the data of this study were obtained using only one cell line (mEC25). In the future, more murine ESCC cell lines will be used to confirm our findings if possible. Moreover, in future studies, we would pay more attention to abscopal effect caused by radioimmunotherapy and the involved mechanisms. In addition, the role of TDLN in the anti-tumor effect of radioimmunotherapy needs to be further clarified.

Overall, our study showed that radiotherapy combined with PD-L1 inhibitors is a promising treatment option for ESCC by establishing the immunostimulatory tumor microenvironment. We hope that these preclinical data in our study may provide novel insights into the design or interpretation of clinical studies on radioimmunotherapy.

Conclusions

Together, our study highlighted the combination of radiotherapy combined with PD-L1 inhibitor as a promising strategy for the treatment of ESCC due to the establishment of an immunostimulatory tumor microenvironment.

Abbreviations

CTLA-4	Cytotoxic T-lymphocyte antigen 4
CXCL	CXC-chemokine ligand
CXCR	CXC-chemokine receptor
DAMPs	Danger-associated molecular patterns
DC	Dendritic cell
ESCC	Esophageal squamous cell carcinoma
GZMB	Granzyme B
IACUC	Institutional Animal Care and Use Committees
ICB	Immune checkpoint blockade
ICI	Immune checkpoint inhibitors
IFN-γ	Interferon gamma
IHC	Immunohistochemical
MDSCs	Myeloid-derived suppressor cells
PBS	Phosphate-buffered saline
PCR	Polymerase chain reaction
PD-1	Programmed cell death protein 1
PD-L1	Programmed death-ligand 1

RT	Radiotherapy
TAMs	Tumor-associated macrophages
T_{CM}	Central memory CD8 + T cells
TILs	Tumor-infiltrating lymphocytes
TME	Tumor-micro-environment
TMB	Tumor mutation burden
Tregs	Regulatory T cells
TDLN	Tumor draining lymph node

Supplementary Information

The online version contains supplementary material available at https://doi.org/10.1186/s12885-025-13801-0.

Supplementary Material 1.

Acknowledgements
We thank the staff of Hangzhou Cancer Institution, Affiliated Hangzhou Cancer Hospital, for their technical support.

Authors' contributions
DQH, ZHF, TRJ and ZK conceived and supervised the experiments. The experiments were performed by YZH, YQQ, YJ and WYP. YZH, YQQ and ZHF interpreted the results of the experiments. YZH and ZK completed the manuscript. All authors read and approved the final manuscript.

Funding
This study was supported by Clinical Research Fund Project of Zhejiang Medical Association (2021ZYC-Z05), Zhejiang Province Health Department Project(2022KY101), "Great Medical Sincerity" cancer prevention and treatment research and academic exchange public welfare program, Hangzhou Agricultural and social Development Research Project(2020ZDSJ0552) and Zhejiang medicine and health science and technology project (2023KY193 and 2024KY204).

Data availability
The datasets uesd and/or analysed during this current study available from the corresponding author on reasonable request.

Declarations

Ethics approval and consent to participate
All of the animal experiments were approved by the Institutional Animal Care and Use Committee (IACUC 20010652), Zhejiang Center of Laboratory Animals(ZJCLA).

Consent for publication
Not applicable.

Competing interests
The authors declare no competing interests.

Author details
[1]Department of Radiation Oncology, Affiliated Hangzhou Cancer Hospital, Hangzhou 310002, China. [2]Hangzhou Cancer Institution, Affiliated Hangzhou Cancer Hospital, Hangzhou 310002, China. [3]Hyperthermia Center, Affiliated Hangzhou Cancer Hospital, Hangzhou 310002, China. [4]Zhejiang Cancer Hospital, Hangzhou, Zhejiang 310022, China.

Received: 21 August 2024 Accepted: 24 February 2025
Published online: 14 March 2025

References

1. Sung H, Ferlay J, Siegel RL, Laversanne M, Soerjomataram I, Jemal A, Bray F. Global Cancer Statistics 2020: GLOBOCAN Estimates of Incidence and Mortality Worldwide for 36 Cancers in 185 Countries. CA Cancer J Clin. 2021;71:209–49. https://doi.org/10.3322/caac.21660.
2. Jiang M, Hu Y, Lin G, Chen C, Li H. Radiotherapy combined with immune checkpoint inhibitors in locally advanced/metastatic esophageal squamous cell carcinoma: clinical trials, efficacy and future directions. Front Immunol. 2023;14:1177085. https://doi.org/10.3389/fimmu.2023.1177085.
3. Hulshof M, Geijsen ED, Rozema T, et al. Randomized Study on Dose Escalation in Definitive Chemoradiation for Patients With Locally Advanced Esophageal Cancer (ARTDECO Study). J Clin Oncol. 2021;39:2816–24. https://doi.org/10.1200/jco.20.03697.
4. Xu Y, Dong B, Zhu W, et al. A Phase III Multicenter Randomized Clinical Trial of 60 Gy versus 50 Gy Radiation Dose in Concurrent Chemoradiotherapy for Inoperable Esophageal Squamous Cell Carcinoma. Clin Cancer Res. 2022;28:1792–9. https://doi.org/10.1158/1078-0432.Ccr-21-3843.
5. Chen Y, Ye J, Zhu Z, et al. Comparing Paclitaxel Plus Fluorouracil Versus Cisplatin Plus Fluorouracil in Chemoradiotherapy for Locally Advanced Esophageal Squamous Cell Cancer: A Randomized, Multicenter, Phase III Clinical Trial. J Clin Oncol. 2019;37:1695–703. https://doi.org/10.1200/jco.18.02122.
6. Sun JM, Shen L, Shah MA, et al. Pembrolizumab plus chemotherapy versus chemotherapy alone for first-line treatment of advanced oesophageal cancer (KEYNOTE-590): a randomised, placebo-controlled, phase 3 study. Lancet. 2021;398:759–71. https://doi.org/10.1016/s0140-6736(21)01234-4.
7. Luo H, Lu J, Bai Y, et al. Effect of Camrelizumab vs Placebo Added to Chemotherapy on Survival and Progression-Free Survival in Patients With Advanced or Metastatic Esophageal Squamous Cell Carcinoma: The ESCORT-1st Randomized Clinical Trial. JAMA. 2021;326:916–25. https://doi.org/10.1001/jama.2021.12836.
8. Demaria S, Coleman CN, Formenti SC. Radiotherapy: Changing the Game in Immunotherapy. Trends Cancer. 2016;2:286–94. https://doi.org/10.1016/j.trecan.2016.05.002.
9. Filatenkov A, Baker J, Mueller AM, et al. Ablative Tumor Radiation Can Change the Tumor Immune Cell Microenvironment to Induce Durable Complete Remissions. Clin Cancer Res. 2015;21:3727–39. https://doi.org/10.1158/1078-0432.Ccr-14-2824.
10. Burnette BC, Liang H, Lee Y, Chlewicki L, Khodarev NN, Weichselbaum RR, Fu YX, Auh SL. The efficacy of radiotherapy relies upon induction of type i interferon-dependent innate and adaptive immunity. Cancer Res. 2011;71:2488–96. https://doi.org/10.1158/0008-5472.Can-10-2820.
11. Wang L, Lynch C, Pitroda SP, Piffkó A, Yang K, Huser AK, Liang HL, Weichselbaum RR. Radiotherapy and immunology. J Exp Med. 2024;221. https://doi.org/10.1084/jem.20232101.
12. Deng L, Liang H, Burnette B, Beckett M, Darga T, Weichselbaum RR, Fu YX. Irradiation and anti-PD-L1 treatment synergistically promote antitumor immunity in mice. J Clin Invest. 2014;124:687–95. https://doi.org/10.1172/jci67313.
13. Dovedi SJ, Adlard AL, Lipowska-Bhalla G, et al. Acquired resistance to fractionated radiotherapy can be overcome by concurrent PD-L1 blockade. Cancer Res. 2014;74:5458–68. https://doi.org/10.1158/0008-5472.Can-14-1258.
14. Tian L, Goldstein A, Wang H, et al. Mutual regulation of tumour vessel normalization and immunostimulatory reprogramming. Nature. 2017;544:250–4. https://doi.org/10.1038/nature21724.
15. Zheng X, Fang Z, Liu X, et al. Increased vessel perfusion predicts the efficacy of immune checkpoint blockade. J Clin Invest. 2018;128:2104–15. https://doi.org/10.1172/jci96582.
16. Wang H, Lin X, Luo Y, et al. α-PD-L1 mAb enhances the abscopal effect of hypo-fractionated radiation by attenuating PD-L1 expression and inducing CD8(+) T-cell infiltration. Immunotherapy. 2019;11:101–18. https://doi.org/10.2217/imt-2018-0049.
17. Gong X, Li X, Jiang T, Xie H, Zhu Z, Zhou F, Zhou C. Combined Radiotherapy and Anti-PD-L1 Antibody Synergistically Enhances Antitumor Effect in Non-Small Cell Lung Cancer. J Thorac Oncol. 2017;12:1085–97. https://doi.org/10.1016/j.jtho.2017.04.014.
18. Lugade AA, Moran JP, Gerber SA, Rose RC, Frelinger JG, Lord EM. Local radiation therapy of B16 melanoma tumors increases the generation of tumor antigen-specific effector cells that traffic to the tumor. J Immunol. 2005;174:7516–23. https://doi.org/10.4049/jimmunol.174.12.7516.
19. Oweida A, Hararah MK, Phan A, et al. Resistance to Radiotherapy and PD-L1 Blockade Is Mediated by TIM-3 Upregulation and Regulatory T-Cell Infiltration. Clin Cancer Res. 2018;24:5368–80. https://doi.org/10.1158/1078-0432.Ccr-18-1038.

20. Oweida A, Lennon S, Calame D, et al. Ionizing radiation sensitizes tumors to PD-L1 immune checkpoint blockade in orthotopic murine head and neck squamous cell carcinoma. Oncoimmunology. 2017;6:e1356153.
21. Dudzinski SO, Cameron BD, Wang J, Rathmell JC, Giorgio TD, Kirschner AN. Combination immunotherapy and radiotherapy causes an abscopal treatment response in a mouse model of castration resistant prostate cancer. J Immunother Cancer. 2019;7:218. https://doi.org/10.1186/s40425-019-0704-z.
22. Philippou Y, Sjoberg HT, Murphy E, et al. Impacts of combining anti-PD-L1 immunotherapy and radiotherapy on the tumour immune microenvironment in a murine prostate cancer model. Br J Cancer. 2020;123:1089–100. https://doi.org/10.1038/s41416-020-0956-x.
23. Azad A, Yin Lim S, D'Costa Z, et al. PD-L1 blockade enhances response of pancreatic ductal adenocarcinoma to radiotherapy. EMBO Mol Med. 2017;9:167–80. https://doi.org/10.15252/emmm.201606674.
24. Close B, Banister K, Baumans V, et al. Recommendations for euthanasia of experimental animals: Part 1. DGXI of the European Commission. Lab Anim. 1996;30:293–316. https://doi.org/10.1258/002367796780739871.
25. Pang D, Laferriere C. Review of Intraperitoneal Injection of Sodium Pentobarbital as a Method of Euthanasia in Laboratory Rodents. J Am Assoc Lab Anim Sci. 2020;59:346. https://doi.org/10.30802/aalas-jaalas-19-000081.
26. Rompré-Brodeur A, Shinde-Jadhav S, Ayoub M, Piccirillo CA, Seuntjens J, Brimo F, Mansure JJ, Kassouf W. PD-1/PD-L1 Immune Checkpoint Inhibition with Radiation in Bladder Cancer. In Situ and Abscopal Effects. Mol Cancer Ther. 2020;19:211–20. https://doi.org/10.1158/1535-7163.Mct-18-0986.
27. Lugade AA, Sorensen EW, Gerber SA, Moran JP, Frelinger JG, Lord EM. Radiation-induced IFN-gamma production within the tumor microenvironment influences antitumor immunity. J Immunol. 2008;180:3132–9. https://doi.org/10.4049/jimmunol.180.5.3132.
28. Tuttle TM, McCrady CW, Inge TH, Salour M, Bear HD. gamma-Interferon plays a key role in T-cell-induced tumor regression. Cancer Res. 1993;53:833–9.
29. Karin N. CXCR3 Ligands in Cancer and Autoimmunity, Chemoattraction of Effector T Cells, and Beyond. Front Immunol. 2020;11:976. https://doi.org/10.3389/fimmu.2020.00976.
30. Borden EC. Interferons α and β in cancer: therapeutic opportunities from new insights. Nat Rev Drug Discov. 2019;18:219–34. https://doi.org/10.1038/s41573-018-0011-2.
31. Lee AJ, Ashkar AA. The Dual Nature of Type I and Type II Interferons. Front Immunol. 2018;9:2061. https://doi.org/10.3389/fimmu.2018.02061.
32. Gerber SA, Sedlacek AL, Cron KR, Murphy SP, Frelinger JG, Lord EM. IFN-γ mediates the antitumor effects of radiation therapy in a murine colon tumor. Am J Pathol. 2013;182:2345–54. https://doi.org/10.1016/j.ajpath.2013.02.041.
33. Hashimoto H, Ueda R, Narumi K, Heike Y, Yoshida T, Aoki K. Type I IFN gene delivery suppresses regulatory T cells within tumors. Cancer Gene Ther. 2014;21:532–41. https://doi.org/10.1038/cgt.2014.60.
34. Fuertes MB, Kacha AK, Kline J, Woo SR, Kranz DM, Murphy KM, Gajewski TF. Host type I IFN signals are required for antitumor CD8+ T cell responses through CD8{alpha}+ dendritic cells. J Exp Med. 2011;208:2005–16. https://doi.org/10.1084/jem.20101159.
35. Jacquelot N, Roberti MP, Enot DP, et al. Predictors of responses to immune checkpoint blockade in advanced melanoma. Nat Commun. 2017;8:592. https://doi.org/10.1038/s41467-017-00608-2.
36. Twyman-Saint Victor C, Rech AJ, Maity A, et al. Radiation and dual checkpoint blockade activate non-redundant immune mechanisms in cancer. Nature. 2015;520:373–7. https://doi.org/10.1038/nature14292.
37. Xiong H, Mittman S, Rodriguez R, Moskalenko M, Pacheco-Sanchez P, Yang Y, Nickles D, Cubas R. Anti-PD-L1 Treatment Results in Functional Remodeling of the Macrophage Compartment. Cancer Res. 2019;79:1493–506. https://doi.org/10.1158/0008-5472.Can-18-3208.
38. Seifert L, Werba G, Tiwari S, et al. Radiation Therapy Induces Macrophages to Suppress T-Cell Responses Against Pancreatic Tumors in Mice. Gastroenterology. 2016;150:1659-72.e5. https://doi.org/10.1053/j.gastro.2016.02.070.
39. Hartley GP, Chow L, Ammons DT, Wheat WH, Dow SW. Programmed Cell Death Ligand 1 (PD-L1) Signaling Regulates Macrophage Proliferation and Activation. Cancer Immunol Res. 2018;6:1260–73. https://doi.org/10.1158/2326-6066.Cir-17-0537.
40. Jones KI, Tiersma J, Yuzhalin AE, Gordon-Weeks AN, Buzzelli J, Im JH, Muschel RJ. Radiation combined with macrophage depletion promotes adaptive immunity and potentiates checkpoint blockade. EMBO Mol Med. 2018;10. https://doi.org/10.15252/emmm.201809342.
41. Sheng H, Huang Y, Xiao Y, et al. ATR inhibitor AZD6738 enhances the antitumor activity of radiotherapy and immune checkpoint inhibitors by potentiating the tumor immune microenvironment in hepatocellular carcinoma. J Immunother Cancer. 2020;8. https://doi.org/10.1136/jitc-2019-000340.
42. Newton JM, Hanoteau A, Liu HC, et al. Immune microenvironment modulation unmasks therapeutic benefit of radiotherapy and checkpoint inhibition. J Immunother Cancer. 2019;7:216. https://doi.org/10.1186/s40425-019-0698-6.
43. Blackburn SD, Shin H, Freeman GJ, Wherry EJ. Selective expansion of a subset of exhausted CD8 T cells by alphaPD-L1 blockade. Proc Natl Acad Sci U S A. 2008;105:15016–21. https://doi.org/10.1073/pnas.0801497105.
44. Budimir N, Thomas GD, Dolina JS, Salek-Ardakani S. Reversing T-cell Exhaustion in Cancer: Lessons Learned from PD-1/PD-L1 Immune Checkpoint Blockade. Cancer Immunol Res. 2022;10:146–53. https://doi.org/10.1158/2326-6066.Cir-21-0515.
45. Ando S, Araki K. CD8 T-cell heterogeneity during T-cell exhaustion and PD-1-targeted immunotherapy. Int Immunol. 2022;34:571–7. https://doi.org/10.1093/intimm/dxac038.
46. Hanna BS, Llaó-Cid L, Iskar M, et al. Interleukin-10 receptor signaling promotes the maintenance of a PD-1(int) TCF-1(+) CD8(+) T cell population that sustains anti-tumor immunity. Immunity. 2021;54:2825-41.e10. https://doi.org/10.1016/j.immuni.2021.11.004.
47. Liu Z, Yu Z, Chen D, et al. Pivotal roles of tumor-draining lymph nodes in the abscopal effects from combined immunotherapy and radiotherapy. Cancer Commun (Lond). 2022;42:971–86. https://doi.org/10.1002/cac2.12348.
48. Fransen MF, Schoonderwoerd M, Knopf P, Camps MG, Hawinkels LJ, Kneilling M, van Hall T, Ossendorp F. Tumor-draining lymph nodes are pivotal in PD-1/PD-L1 checkpoint therapy. JCI Insight. 2018;3. https://doi.org/10.1172/jci.insight.124507.

Publisher's Note